


## PAPER

[View Article Online](#)  
[View Journal](#) | [View Issue](#)Cite this: *Anal. Methods*, 2024, 16, 8157

# Turn-on fluorescent probe based on dicyanoisophorone for bioimaging and rapid detection of peroxynitrite in aqueous media†

Jianwei Wu, Jia Li, Yaqiao Shi, Liting Jiang, Chenming Chan, Ru Feng,\* Yue Wang and Zhaoli Xue \*

A novel dicyanoisophorone-based colorimetric fluorescent probe **3** has been prepared for recognizing peroxynitrite in aqueous conditions. A large bathochromic shift of the absorption band is observed upon titration with  $\text{ONOO}^-$ , inducing a clearly visible solution color change from yellow to pale pink, which makes “naked-eye” detection possible. Moreover, probe **3** can react instantly with  $\text{ONOO}^-$  and is accompanied by a significant fluorescence enhancement at 621 nm while the detection limit is as low as 37 nM. Most importantly, probe **3** exhibits high selectivity and sensitivity towards  $\text{ONOO}^-$  in the presence of other competitive ions in aqueous solution. Probe **3** has also been successfully applied in living MCF-7 cells, and the results suggest that probe **3** could be applied as a potential candidate for the detection of  $\text{ONOO}^-$ .

Received 19th September 2024  
Accepted 27th October 2024

DOI: 10.1039/d4ay01721h

[rsc.li/methods](https://rsc.li/methods)

## Introduction

It is well known that reactive oxygen species (ROS) are involved in the redox balance of organisms, including hydrogen peroxide ( $\text{H}_2\text{O}_2$ ), hypochlorous acid ( $\text{HClO}$ ), hypochlorite ( $\text{ClO}^-$ ), peroxynitrite ( $\text{ONOO}^-$ ), superoxide ( $\text{O}_2^{\cdot-}$ ), hydroxyl radicals ( $\cdot\text{OH}$ ), and peroxy radicals ( $\text{ROO}^{\cdot}$ ).<sup>1–3</sup> Among those species, peroxynitrite, possessing considerable oxidation and nitrification capacity, is deemed to be a more reactive species compared to its parent molecules, namely nitric oxide (NO) and superoxide ( $\text{O}_2^{\cdot-}$ ).<sup>4–7</sup> Based on its oxidation and nitrification ability, peroxynitrite has been identified as a principal factor for causing cardiovascular, neurodegenerative, and inflammatory diseases.<sup>4,5,8–16</sup> As a result, effective methods for the detection of peroxynitrite have received great attention.

Peroxyntirite differs from common ions in that it arises and exists in living organisms; however, owing to its short lifetime, high reactivity, and low concentration, the detection of peroxynitrite is more challenging than for common ions. To date, common detection methods such as immunohistochemistry, fluorescence, chemiluminescence and electrochemical technology have been investigated.<sup>12,17–19</sup> Among the aforementioned methodologies, the fluorogenic method is one of the most attractive due to its high selectivity, fast response time, high sensitivity, low-cost equipment, and convenient protocol.<sup>19–22</sup> Reported  $\text{ONOO}^-$  fluorescent probes generally

utilize the ability of  $\text{ONOO}^-$  to oxidize chalcogenides,<sup>23</sup> boronic acids,<sup>24</sup> hydrazides,<sup>25</sup> and others.<sup>26</sup> However, there are few reports focused on the detection of peroxynitrite through the oxidation of phenolic hydroxyl groups in molecules with the isophorone system.

In this paper, we report a novel colorimetric fluorescent probe **3** that uses a phenolic hydroxyl group as the response group for recognizing  $\text{ONOO}^-$  in aqueous conditions. Probe **3** shows one intense absorbance band at 697 nm and possesses a large Stokes shift around 183 nm. When titrated with  $\text{ONOO}^-$ , probe **3** exhibited a noticeable bathochromic-shift, from 438 nm to 697 nm, along with a solution color change from orange to pale pink. Furthermore, there was a remarkable enhancement of the fluorescence intensity at 621 nm upon titration with  $\text{ONOO}^-$ , thus making it a “turn-on” fluorescent probe able to detect  $\text{ONOO}^-$  in aqueous conditions. Meanwhile, probe **3** exhibits a fast response and low detection limit (37 nM). Additionally, an MTT experiment indicated that the probe has low cytotoxicity and good biocompatibility. Probe **3** was applied in the fluorescence imaging of MCF-7 cells, verifying that the detection of  $\text{ONOO}^-$  at the cellular level is possible.

## Experimental

### Synthesis of 4,4'-dihydroxy-[1,1'-biphenyl]-3,3'-dicarbaldehyde **2**

4,4'-Dihydroxybiphenyl (2.12 g, 10.74 mmol) and methenamine (3.02 g, 21.48 mmol) were added into a 250 mL round-bottom flask. To this flask, trifluoroacetic (75.3  $\mu\text{L}$ , 1.01  $\mu\text{mol}$ ) was injected, and the mixture was stirred for 3.0 h at 70 °C under an  $\text{N}_2$  atmosphere. Further, 100 mL of cold water was added, and

School of Chemistry and Chemical Engineering, Jiangsu University, Zhenjiang 212013, PR China. E-mail: fengru@ujs.edu.cn; zhaolixue@ujs.edu.cn

† Electronic supplementary information (ESI) available. See DOI: <https://doi.org/10.1039/d4ay01721h>

the mixture was stirred for another 3.0 h at room temperature. When the reaction was finished, the organic phase was extracted using ethyl acetate (2 × 30 mL). The organic solution was combined, dried over anhydrous Na<sub>2</sub>SO<sub>4</sub> and then concentrated to obtain the crude product. This crude product was further purified *via* column chromatography (silica gel, CH<sub>2</sub>Cl<sub>2</sub>/petroleum ether = 3:1) to obtain a yellow solid. Yield: 0.44 g, 17.1%. M.p.: 185–188 °C. <sup>1</sup>H NMR (400 MHz, DMSO-*d*<sub>6</sub>, 298 K) δ = 10.80 (s, 2 H, aldehyde), 10.30 (s, 2 H, hydroxy), 7.88 (s, 2 H, phenyl), 7.80 (d, *J* = 8.6 Hz, 2H, phenyl), 7.07 (d, *J* = 8.6 Hz, 2 H, phenyl) ppm. <sup>13</sup>C NMR (100 MHz, DMSO-*d*<sub>6</sub>, 298 K) δ = 192.4, 160.4, 130.8, 126.9, 122.8, 118.6 ppm.

### Synthesis of chemosensor 3

Compound **1** (0.5 g, 2.7 mmol) and **2** (0.32 g, 1.35 mmol) were added into a 100 mL two-neck round-bottom flask under an N<sub>2</sub> atmosphere. Then, CH<sub>3</sub>CN (15 mL) and piperidine (0.15 mL, 1.52 mmol) were added slowly. After that, the mixture was stirred and refluxed while the reaction was monitored using TLC until the raw material was totally consumed. Further, the crude product was extracted from the mixture using ethyl acetate (2 × 30 mL), washing with water and drying over anhydrous Na<sub>2</sub>SO<sub>4</sub> before concentrating under reduced pressure to get the crude product. This crude product was further purified using column chromatography (silica gel, CH<sub>2</sub>Cl<sub>2</sub>/petroleum ether = 5:1) to obtain the target product as a red solid. Yield: 0.41 g, 45.9%. M.p.: 245–250 °C. <sup>1</sup>H NMR (400 MHz, DMSO-*d*<sub>6</sub>, 298 K) δ = 10.19 (s, 2 H, hydroxy), 7.94 (s, 2 H, vinyl), 7.50 (s, 6 H, phenyl), 6.96 (d, *J* = 8.5 Hz, 2 H, vinyl), 6.87 (s, 2 H, vinyl), 2.60 (s, 4H, methylene), 2.54 (s, 4 H, methylene), 1.02 (s, 12 H, -CH<sub>3</sub>) ppm. <sup>13</sup>C NMR (100 MHz, DMSO-*d*<sub>6</sub>, 298 K) δ = 170.8, 156.9, 155.1, 133.7, 131.8, 129.5, 125.4, 123.6, 122.7, 116.9, 114.6, 113.6, 76.5, 42.8, 38.8, 32.5, 27.9 ppm. UV-vis (in DMSO) λ [nm] (ε [M<sup>-1</sup> cm<sup>-1</sup>]): 438 (44 776). HR MS-MALDI TOF (*m/z*): calcd for C<sub>46</sub>H<sub>36</sub>N<sub>4</sub>O [M + H<sup>+</sup>]: 661.2967, found: 661.2961.

## Result and discussion

### Synthesis and characterization

To construct a sensitive NIR fluorescent probe for ONOO<sup>-</sup>, isophorone was chosen as the NIR fluorophore due to its large Stokes shift and low cytotoxicity. Usually, the phenol group in fluorescent sensors is utilized as the response site for the ClO<sup>-</sup>

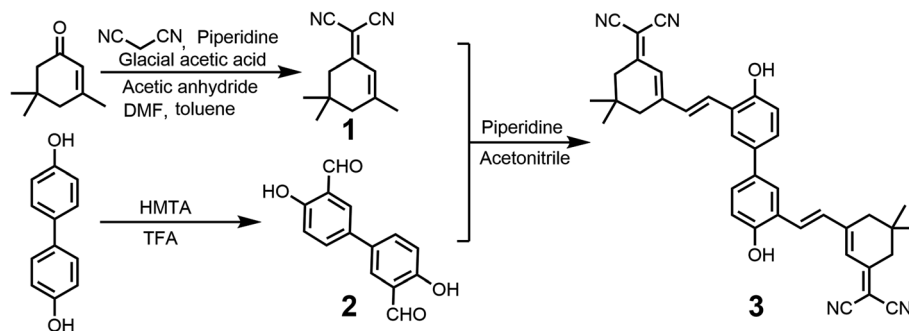
ion based on its reported strong reduction properties.<sup>27,28</sup> However, in this paper, we introduced two phenol groups to the 4,4'-positions of biphenyl with the aim of detecting ONOO<sup>-</sup> while two isophorone groups were added to the 3,3'-position to obtain probe **3** (Scheme 1). Probe **3** exhibited weak fluorescence before encountering the ONOO<sup>-</sup> ion, mainly due to intramolecular charge transfer (ICT) between the isophorone groups and the biphenol group. Once the probe was oxidized using ONOO<sup>-</sup>, the phenolic hydroxyl groups transformed into a benzoquinone, thus blocking the ICT process while the fluorescence intensity was restored.

Compound **2** was synthesized through a Duff reaction, while probe **3** was prepared *via* a conventional condensation strategy between compound **1** and **2** with moderate yield. The structure of probe **3** was verified using <sup>1</sup>H NMR, <sup>13</sup>C NMR and HR MS spectroscopy (Fig. S1–S8†). UV-vis and fluorescence spectroscopic experiments in common solvents have been conducted (Fig. S9–S11†). The results revealed that for probe **3**, the absorption spectra showed a few differences, while the emission spectra exhibited significant changes in different common solvents. This finding indicated that the fluorescent properties of probe **3** relied quite a bit on the polarity of the solvent. Furthermore, a large Stokes shift was found for probe **3** (cal. as 183 nm), which makes the probe a good candidate for fluorescent biological investigations (Fig. S9†).

### UV-vis and fluorescence spectroscopic titration studies

The UV-vis spectroscopic changes of probe **3** (18.0 μM) upon titration with different concentration of ONOO<sup>-</sup> in DMSO–H<sub>2</sub>O (*v:v* = 9:1; HEPES 10 mM, pH = 7.2) were investigated. As shown in Fig. 1a, probe **3** exhibited only one absorption band at 438 nm. As the concentration of ONOO<sup>-</sup> increased, the absorbance peak gradually decreased while two new absorbance peaks around 326 nm and 697 nm appeared, which might be due to the oxidation of the phenolic hydroxyl groups. Meanwhile, the solution color changed from yellow to pale pink, a change which can be observed by the naked eye (Fig. 2c). Additionally, there is a good linear relationship between the concentration of ONOO<sup>-</sup> and the ratio of the absorbance at 438 nm to 697 nm (Fig. 1b).

Furthermore, the fluorescence spectroscopic response of probe **3** (18.0 μM) was also examined by titrating ONOO<sup>-</sup> in DMSO–H<sub>2</sub>O (*v:v* = 9:1; HEPES 10 mM, pH = 7.2). As shown in



Scheme 1 Synthesis of probe **3**.

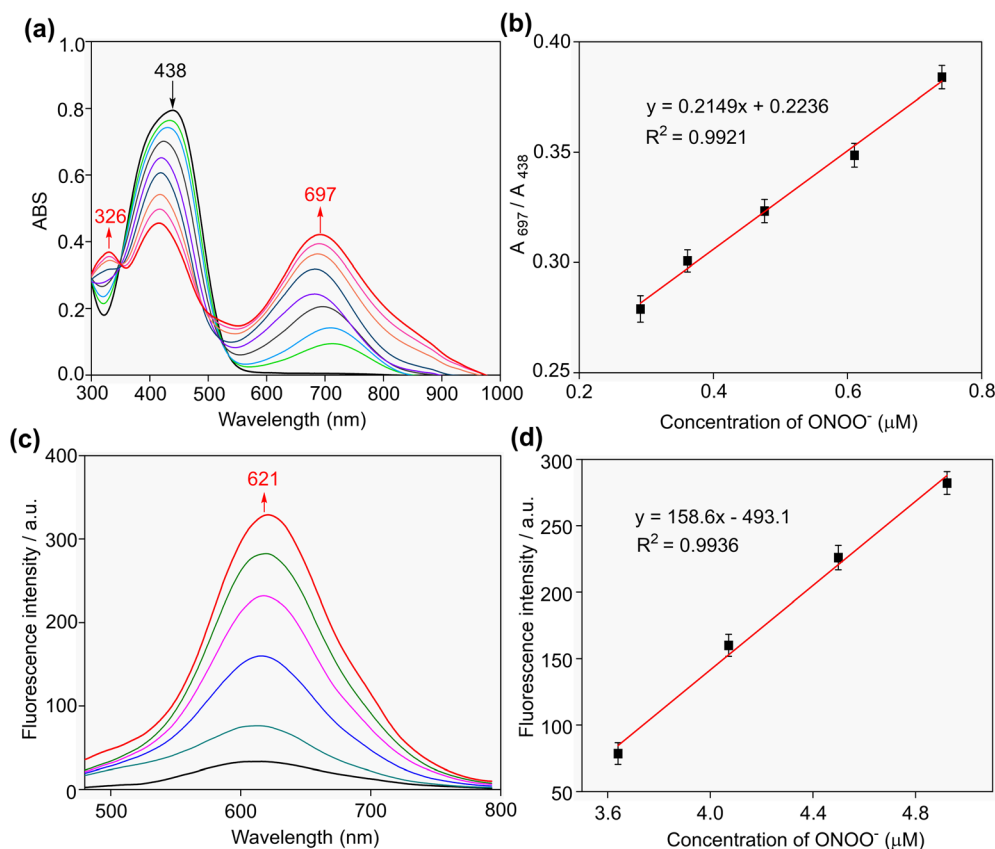


**Fig. 1** (a) UV-vis absorption spectra of probe **3** upon titration with ONOO<sup>-</sup> (0–1.4 μM) at various concentrations in DMSO–H<sub>2</sub>O (v : v = 9 : 1; HEPES 10 mM, pH = 7.2); (b) absorbance ratios ( $A_{697}/A_{438}$ ) of probe **3** as a function of different ONOO<sup>-</sup> concentrations; (c) fluorescence emission spectra of probe **3** upon titration with ONOO<sup>-</sup> in DMSO–H<sub>2</sub>O (v : v = 9 : 1; HEPES 10 mM, pH = 7.2); and (d) the relationship between the concentration of ONOO<sup>-</sup> and the fluorescence intensity at 621 nm based on fluorescence titration experiments. The excitation wavelength was 438 nm.

Fig. 1c, a remarkable enhancement of the fluorescence intensity at 621 nm was found upon the addition of ONOO<sup>-</sup>, thus demonstrating the turn-on fluorescent properties of probe **3**. Such an enhancement of the fluorescence intensity is likely due to the oxidation of the phenolic hydroxyl groups, thus halting the ICT process and restoring the fluorescence intensity. At the end of the titration, the solution showed strong pink fluorescence under a 365 nm UV-lamp (Fig. 3c). Analysis of the titration data showed that the fluorescence intensity has a good linear relationship with the concentration of ONOO<sup>-</sup> (Fig. 1d). According to formula  $LOD = 3\sigma/k$ , the ONOO<sup>-</sup> detection limit of probe **3** was calculated to be as low as 37 nM.

### Selectivity and sensitivity studies

To test the selectivity of probe **3** towards ONOO<sup>-</sup>, different kinds of competitive ROS (H<sub>2</sub>O<sub>2</sub>, <sup>•</sup>OH, ROO<sup>-</sup>, O<sub>2</sub><sup>•-</sup>, ClO<sup>-</sup>) and oxidative metal ions (Cu<sup>2+</sup>, Fe<sup>3+</sup>, Ag<sup>+</sup>, Hg<sup>2+</sup>) were investigated (Fig. 2). As shown in Fig. 2, only the addition of ONOO<sup>-</sup> reduces the absorbance peak at 438 nm while other competitive ROS together with oxidative metal ions have negligible influence. At the same time, the naked eye could easily distinguish ONOO<sup>-</sup> from other interfering species. Such results demonstrate that probe **3** exhibits a highly selective response for ONOO<sup>-</sup>. More

importantly, the presence of other competitive ROS together with oxidative ions did not affect the recognition of ONOO<sup>-</sup> by probe **3**.

Furthermore, the capability of probe **3** to detect ONOO<sup>-</sup> in the presence of other interfering species could be verified through a fluorescence interference investigation under the same conditions. As illustrated in Fig. 3, only the addition of ONOO<sup>-</sup> enhanced the fluorescence intensity remarkably at 621 nm, while the other ROS and oxidative metal ions caused negligible fluctuations in the fluorescence intensity, even at concentrations below 1.0 mM.

### Reaction time, pH effect and imaging stability

The response time of a probe is a crucial indicator of its real-time detection capability. The time-dependent fluorescence intensity response of probe **3** to ONOO<sup>-</sup> was then explored (Fig. S12†). In the presence of ONOO<sup>-</sup>, the fluorescence intensity of probe **3** significantly increased and reached a constant strength at 621 nm within less than 5 s. These results reveal that probe **3** could be applied for the rapid detection of ONOO<sup>-</sup> in biological environments. Furthermore, probe **3** could maintain its fluorescence intensity with negligible changes after 10 min. To explore the appropriate pH range for probe **3** to effectively

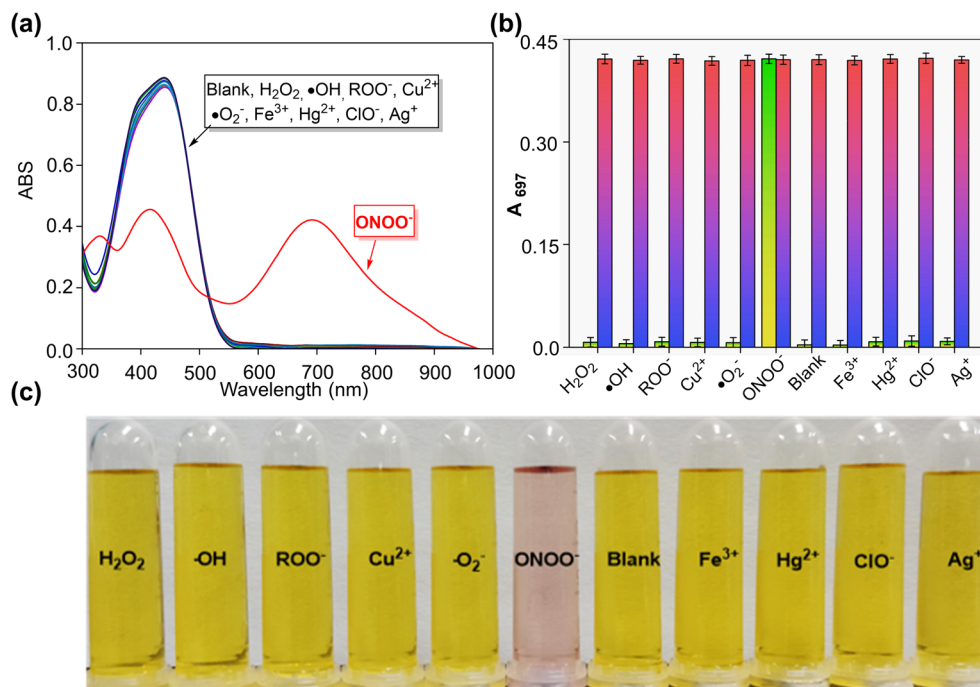


Fig. 2 (a) UV-vis absorption performance of probe **3** (5.0  $\mu\text{M}$ ) with various ROS and oxidative ions (1.0 mM) in DMSO–H<sub>2</sub>O (v : v = 9 : 1; HEPES 10 mM, pH = 7.2); (b) absorbance intensity of selected different ROS and oxidative ions; (c) and photographs of probe **3** upon adding a variety of ROS and oxidative ions under sunlight.

detect ONOO<sup>−</sup>, the effect of pH on probe **3** with and without the presence of ONOO<sup>−</sup> was investigated (Fig. S13<sup>†</sup>). According to Fig. S13,<sup>†</sup> probe **3** can effectively recognize ONOO<sup>−</sup> in aqueous

conditions in a pH range from 3 to 9, thus verifying that probe **3** has good potential to detect ONOO<sup>−</sup> *in vitro*. Furthermore, as compared to other reported ONOO<sup>−</sup> fluorescent sensors, probe

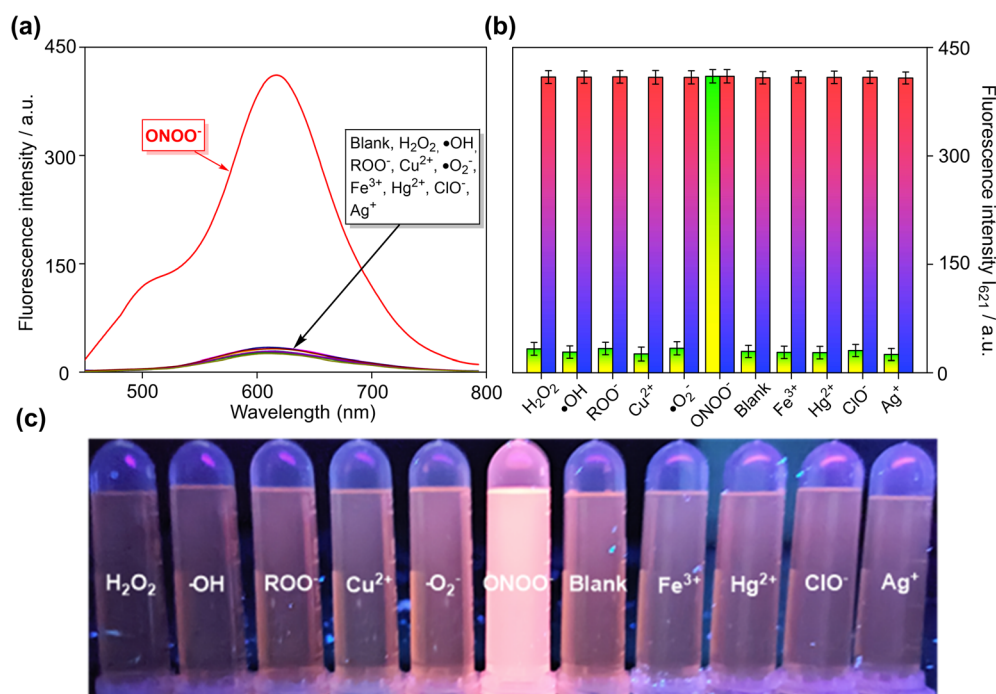


Fig. 3 (a) Changes in the fluorescence emission spectra of probe **3** in the presence of ONOO<sup>−</sup> and other ROS and oxidative metal ions (1.0 mM) in DMSO–H<sub>2</sub>O (v : v = 9 : 1; HEPES 10 mM, pH = 7.2). The excitation wavelength was 438 nm. (b) Fluorescence responses at 621 nm ( $I_{621}$ ) for probe **3** in the presence of ONOO<sup>−</sup> and other ROS and oxidative ions. (c) Photographs of probe **3** upon adding a variety of ROS and oxidative ions under illumination with a 365 nm UV-lamp.



**Table 1** Comparisons of probe **3** with other reported probes for detection of  $\text{ONOO}^-$ 

Entry number	Ex./Em. (nm)	LOD	Response time	Application	Ref.
1	500/670	10 nM	4 min	SH-SY5Y cells	29
2	594/600	3.4 nM	40 min	PC12 cells	30
3	405/720	28 nM	5 min	HepG2 cells	31
4	350/490	9.89 nM	6 min	Mouse	32
5	525/570	212 nM	1 min	HepG2 cells	33
6	570/630	34 nM	240 s	H9c2 cells	34
7	520/685	96 nM	10 min	RAW 264.7 cells	35
8	438/621	37 nM	5 s	MCF-7 cells	This work

**3** exhibited many advantages in terms of its low detection limit, rapid response time and turn-on fluorescence capability (Table 1).

### Response mechanism

To study the mechanism by which probe **3** responds to  $\text{ONOO}^-$ ,  $^1\text{H}$  NMR titration experiments of probe **3** with  $\text{ONOO}^-$  were conducted in  $d_6$ -DMSO solution at room temperature (Fig. S14<sup>†</sup>). The chemical shift of 10.19 ppm could be assigned to the hydroxyl groups, which completely disappeared upon the addition of  $\text{ONOO}^-$ . The result indicated that probe **3** forms a benzoquinone structure through an oxidation process in the presence of  $\text{ONOO}^-$  (Fig. 4b). The mechanism was also confirmed using FTIR and ESI MS (Fig. S15 and S16<sup>†</sup>). A new peak around  $1675\text{ cm}^{-1}$  and an ion peak at  $m/z$  599.2595 (calcd for  $\text{C}_{38}\text{H}_{32}\text{N}_4\text{O}_2\text{Na}$ : 599.2523) both indicated the formation of a benzoquinone structure.

In order to get a deep understanding of the oxidation process that occurs between probe **3** and  $\text{ONOO}^-$ , we carried out density-functional theory (DFT) calculations at the B3LYP/6-31G

level of theory using the Gaussian 09 program (Fig. 4a). After being oxidized by  $\text{ONOO}^-$ , the HOMO and LUMO energy gap of probe **3** significantly decreased from 2.98 eV to 1.71 eV, which is consistent with the variation seen in the UV-vis spectrum upon titration. Additionally, in the newly formed benzoquinone structure, the HOMO electron density was distributed over both the isophorone unit and phenolate unit, which suggests that an enhancement of the  $\pi$ -conjugation in the entire molecule occurs (Fig. 4a).

### Practical application in MCF-7 cells

To explore the application of probe **3** for detecting  $\text{ONOO}^-$  in living cells, the MCF-7 cell line was chosen for fluorescence imaging. First, an MTT investigation was carried out to check the cytotoxicity of probe **3**, and the results verify that it has low toxicity (Fig. S17<sup>†</sup>), even in the presence of a high concentration of probe **3**, and that the MCF-7 cells still maintain a certain activity. As illustrated in Fig. 5, after being treated with probe **3** for 0.5 h, the living MCF-7 cells did not exhibit fluorescence. However, after incubation with increasing concentrations of

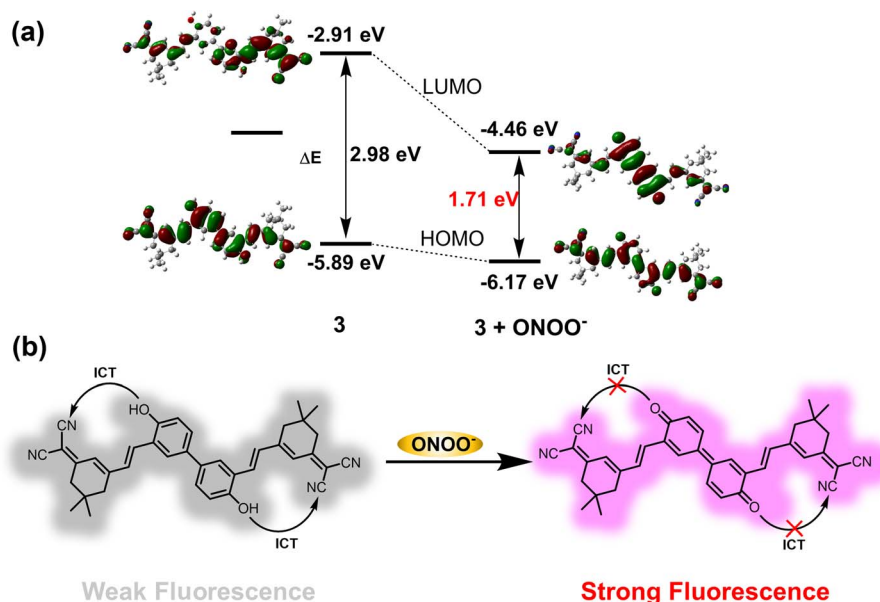


**Fig. 4** (a) HOMO and LUMO energy levels of probe **3** and **3 + ONOO<sup>-</sup>**. (b) The proposed fluorescence mechanism for probe **3** in the presence of  $\text{ONOO}^-$ .

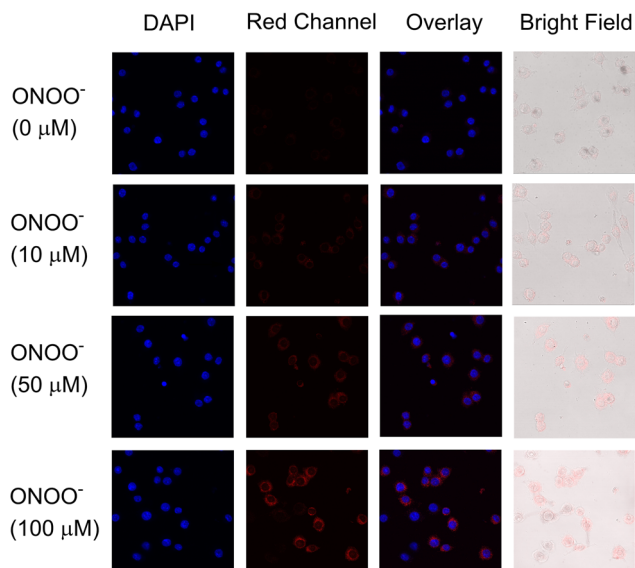


Fig. 5 Fluorescence images of MCF-7 cell after incubation with probe 3 (10  $\mu\text{M}$ ) and different concentrations of  $\text{ONOO}^-$  (0, 10, 50 and 100  $\mu\text{M}$ ).

$\text{ONOO}^-$  for another 0.5 h, the living MCF-7 cells exhibited enhanced red fluorescence, which indicates that probe 3 successfully realizes detection of  $\text{ONOO}^-$  via a “turn-on” switch mode at the cellular level.

## Conclusions

In summary, a dicyanoisophorone-based “turn-on” fluorescent chemosensor, probe 3, was successfully synthesized and applied for the detection of  $\text{ONOO}^-$  in MCF-7 cells. Both UV-vis absorption and emission spectra of the probe showed clear observable color changes upon the addition of  $\text{ONOO}^-$ , while no clear response was observed in the presence of some other competitive ROS and oxidative ions, indicating the excellent selectivity of the probe towards  $\text{ONOO}^-$ . In addition, good linear relationships between the emission intensities of probe 3 and the concentration of  $\text{ONOO}^-$  were found, leading to a low LOD value of 37 nM. The response time of the probe was recorded to be less than 5 s, while the influence of the pH on the intensity was also examined. Moreover, the response mechanism was investigated using a  $^1\text{H}$  NMR titration method, suggesting that the change in fluorescence is due to the oxidation of probe 3 to form a benzoquinone structure that halts the ICT process. The application of the probe was then examined by investigating its fluorescence response in the bioimaging of MCF-7 cells, thus demonstrating the viability of probe 3 as an efficient probe for  $\text{ONOO}^-$  sensing.

## Data availability

The data that support the findings of this study are available from the corresponding author, Zhaoli Xue, upon reasonable request.

## Author contributions

Jianwei Wu: investigation, visualization, writing original draft. Jia Li, Yaqiao Shi, Liting Jiang, Chenming Chan, Yue Wang: conceptualization, methodology, data curation. Ru Feng, Zhaoli Xue: funding acquisition, project administration, resources, supervision, writing – review & editing.

## Conflicts of interest

The authors declare that they have no known competing financial interests or personal relationships that could have appeared to influence the work reported in this paper.

## Acknowledgements

This work was supported by grants from the Natural Science Foundation of Jiangsu Province (BK20190238) and the National Natural Science Foundation of China (No. 22308132). The theoretical calculations were carried out at the Centre for High Performance Computing in Jiangsu University.

## References

- 1 K. Apel and H. Hirt, *Annu. Rev. Plant Biol.*, 2004, **55**, 373–399.
- 2 S. M. Crusz and F. R. Balkwill, *Nat. Rev. Clin. Oncol.*, 2015, **12**, 584–596.
- 3 S. S. Gill and N. Tuteja, *Plant Physiol. Biochem.*, 2010, **48**, 909–930.
- 4 G. Ferrer-Sueta, N. Campolo, M. Trujillo, S. Bartesaghi, S. Carballal, N. Romero, B. Alvarez and R. Radi, *Chem. Rev.*, 2018, **118**, 1338–1408.
- 5 G. Ferrer-Sueta and R. Radi, *ACS Chem. Biol.*, 2009, **4**, 161–177.
- 6 D. Furman, J. Campisi, E. Verdin, P. Carrera-Bastos, S. Targ, C. Franceschi, L. Ferrucci, D. W. Gilroy, A. Fasano, G. W. Miller, A. H. Miller, A. Mantovani, C. M. Weyand, N. Barzilai, J. J. Goronzy, T. A. Rando, R. B. Effros, A. Lucia, N. Kleinstreuer and G. M. Slavich, *Nat. Med.*, 2019, **25**, 1822–1832.
- 7 P. Pacher, J. S. Beckman and L. Liaudet, *Physiol. Rev.*, 2007, **87**, 315–424.
- 8 S. I. Dikalov and D. G. Harrison, *Antioxid. Redox Signaling*, 2014, **20**, 372–382.
- 9 J. N. Fullerton and D. W. Gilroy, *Nat. Rev. Drug Discovery*, 2016, **15**, 551–567.
- 10 Z. Guo, S. Park, J. Yoon and I. Shin, *Chem. Soc. Rev.*, 2014, **43**, 16–29.
- 11 F. L. Heppner, R. M. Ransohoff and B. Becher, *Nat. Rev. Neurosci.*, 2015, **16**, 358–372.
- 12 H. Kobayashi, M. Ogawa, R. Alford, P. L. Choyke and Y. Urano, *Chem. Rev.*, 2010, **110**, 2620–2640.
- 13 H. F. Poon, V. Calabrese, G. Scapagnini and D. A. Butterfield, *Clin. Geriatr. Med.*, 2004, **20**, 329–359.
- 14 M. Z. Tay, C. M. Poh, L. Renia, P. A. MacAry and L. F. P. Ng, *Nat. Rev. Immunol.*, 2020, **20**, 363–374.

- 15 M. Valko, D. Leibfritz, J. Moncol, M. T. D. Cronin, M. Mazur and J. Telser, *Int. J. Biochem. Cell Biol.*, 2006, **39**, 44–84.
- 16 A. A. Zarrin, K. Bao, P. Lupardus and D. Vucic, *Nat. Rev. Drug Discovery*, 2021, **20**, 39–63.
- 17 W. Sun, S. Guo, C. Hu, J. Fan and X. Peng, *Chem. Rev.*, 2016, **116**, 7768–7817.
- 18 C. Szabo, H. Ischiropoulos and R. Radi, *Nat. Rev. Drug Discovery*, 2007, **6**, 662–680.
- 19 W. Zhang, Y. Liu, Q. Gao, C. Liu, B. Song, R. Zhang and J. Yuan, *Chem. Commun.*, 2018, **54**, 13698–13701.
- 20 D. Cheng, J. Peng, Y. Lv, D. Su, D. Liu, M. Chen, L. Yuan and X. Zhang, *J. Am. Chem. Soc.*, 2019, **141**, 6352–6361.
- 21 R. Han, W. Shu, H. Kang, Q. Duan, X. Zhang, C. Liang, M. Gao, L. Xu, J. Jing and X. Zhang, *Anal. Chim. Acta*, 2022, **1203**, 339652.
- 22 D.-Y. Zhou, Y. Li, W.-L. Jiang, Y. Tian, J. Fei and C.-Y. Li, *Chem. Commun.*, 2018, **54**, 11590–11593.
- 23 F. Yu, P. Li, B. Wang and K. Han, *J. Am. Chem. Soc.*, 2013, **135**, 7674–7680.
- 24 J. Kim, J. Park, H. Lee, Y. Choi and Y. Kim, *Chem. Commun.*, 2014, **50**, 9353–9356.
- 25 B. Zhu, M. Zhang, L. Wu, Z. Zhao, C. Liu, Z. Wang, Q. Duan, Y. Wang and P. Jia, *Sens. Actuators, B*, 2018, **257**, 436–441.
- 26 S. Wang, L. Chen, P. Jangili, A. Sharma, W. Li, J.-T. Hou, C. Qin, J. Yoon and J. S. Kim, *Coord. Chem. Rev.*, 2018, **374**, 36–54.
- 27 C. Chan, W. Zhang, Z. Xue, Y. Fang, F. Qiu, J. Pan and J. Tian, *Anal. Chem.*, 2022, **94**, 5918–5926.
- 28 C. Chan, J. Li, Z. Xue and B. Guan, *Anal. Methods*, 2022, **14**, 2311–2317.
- 29 S. Chen, W. Huang, H. Tan, G. Yin, S. Chen, K. Zhao, Y. Huang, Y. Zhang, H. Li and C. Wu, *Analyst*, 2023, **148**, 4331–4338.
- 30 P. Wang, L. Yu, J. Gong, J. Xiong, S. Zi, H. Xie, F. Zhang, Z. Mao, Z. Liu and J. S. Kim, *Angew. Chem., Int. Ed.*, 2022, **61**, e202206894.
- 31 W. Wu, X. Liao, Y. Chen, L. Ji and H. Chao, *Anal. Chem.*, 2021, **93**, 8062–8070.
- 32 Z. Wang, W. Wang, P. Wang, X. Song, Z. Mao and Z. Liu, *Anal. Chem.*, 2021, **93**, 3035–3041.
- 33 L. Wen, X. Ma, J. Yang, M. Jiang, C. Peng, Z. Ma, H. Yu and Y. Li, *Anal. Chem.*, 2022, **94**, 4763–4769.
- 34 Q. Sun, J. Xu, C. Ji, M. S. S. Shaibani, Z. Li, K. Lim, C. Zhang, L. Li and Z. Liu, *Anal. Chem.*, 2020, **92**, 4038–4045.
- 35 X. Luo, Z. Cheng, R. Wang and F. Yu, *Anal. Chem.*, 2021, **93**, 2490–2499.